

# Performance and Variability Optimization Strategies in a Sub-200mV, 3.5pJ/inst, 11nW Subthreshold Processor

Scott Hanson, Bo Zhai, Mingoo Seok, Brian Cline, Kevin Zhou, Meghna Singhal, Michael Minuth, Javin Olson, Leyla Nazhandali, Todd Austin, Dennis Sylvester, David Blaauw, *University of Michigan, Ann Arbor, MI*

## Abstract

A robust, energy efficient subthreshold (sub- $V_{th}$ ) processor has been designed and tested in a 0.13 $\mu$ m technology. The processor consumes 11nW at  $V_{dd}$ =160mV and 3.5pJ/inst at  $V_{dd}$ =350mV. Variability and performance optimization techniques are investigated for sub- $V_{th}$  circuits.

Keywords: subthreshold, variability, body-bias, low power

## Introduction

Recent progress in low voltage circuit design has created opportunities for the development of inexpensive pervasive computing systems. Previous work has shown that minimum energy operation typically occurs in the sub- $V_{th}$  regime ( $V_{dd} < V_{th}$ ) [1,2]. In this work, we describe a sub- $V_{th}$  processor for sensor network applications. The processor consumes 3.5pJ/inst at  $V_{dd}$ =350mV under zero body bias and 11nW at  $V_{dd}$ =160mV under a reverse body bias. There are two primary problems confronting sub- $V_{th}$  designers: increased variability and reduced performance. We use extensive measurements to investigate both of these issues and demonstrate techniques for mitigating these problems. To control variability, we propose a body biasing strategy that leverages the unique sensitivities observed in sub- $V_{th}$  circuits. To address performance, we investigate both chip-level and block-level performance enhancement techniques.

## Design for Energy Efficiency

Sub- $V_{th}$  operation must be accompanied by appropriate architectural design to ensure maximum energy efficiency. We use a simple architecture with 8-bit data and 12-bit instruction word sizes [3]. These word sizes have been chosen to maximize energy efficiency while still meeting the demands of sensor network processing. The core uses a 3-stage pipeline with instruction pre-fetching and branch speculation to reduce the number of clocks per instruction (CPI) and improve energy efficiency. A 1.5kb instruction memory and a 1kb data memory are both implemented using a latch-based memory with mux-based read/write schemes [4]. The processor has been fabricated in a 0.13 $\mu$ m twin-well technology with  $V_{th}$ =400mV at  $V_{ds}$ =50mV. Body biases have been routed in addition to supply rails, as shown in Fig. 2.  $V_{dd}$  and  $V_{ss}$  rails are routed in minimum pitch wires since interconnect resistance is negligible compared to device resistance in the sub- $V_{th}$  regime. Three processor variants, each designed with a different gate sizing strategy, are highlighted in Fig. 3. Proc A uses minimum gate sizes, while Procs B and C (described later) use increased gate widths and lengths along critical paths.

Frequency and energy measurements of Proc A are shown for a typical die in Fig. 4. As predicted by [1,2], energy reaches a minimum due to increased leakage energy at low  $V_{dd}$ . The processor achieves a minimum of 3.5pJ/inst at  $V_{dd}$ =350mV with a frequency of 354kHz. The core (without memories, register file or pre-fetch buffer) reaches a minimum of 515fJ/inst at  $V_{dd}$ =290mV. In power-limited applications, a reverse body bias may be applied. Under a reverse bias of 300mV, the processor consumes 11nW at  $V_{dd}$ =160mV with the core consuming only 735pW. We focus on energy minimization for the remainder of this paper since it is more relevant for battery-powered applications.

## Variability Control

Due to the exponential dependence of sub- $V_{th}$  current on  $V_{th}$ , body biasing is useful for addressing variation in sub- $V_{th}$  circuits. Previous work [5,6] has investigated body biasing, but we focus on its relevance to sub- $V_{th}$  operation. For this discussion, we define two body bias quantities: *differential* ( $V_{diff} = [V_{dd} - V_{B,PFET}] - V_{B,NFET}$ ) and *offset* ( $V_{offset} = V_{B,NFET}$ ).

Matching between PFET and NFET devices, achieved by adjusting the body bias differential, maximizes noise margins in the sub- $V_{th}$  regime. Fig. 5 shows how the minimum functional  $V_{dd}$  ( $V_{dd,limit}$ ), a strong indicator of noise margins [6], is reduced from 180mV to 150mV when applying optimal differential. Fig. 5 also shows that the energy consumption of the core reaches a minimum at nearly the same differential. Though dynamic energy is largely insensitive to differential, leakage energy is minimized at the point where PFET and NFET strengths are matched. Fig. 5 stresses an important point: the differential that maximizes noise margins is almost identical to the differential that minimizes energy. Thus, body bias generation is simplified since the differential may be selected by matching the currents on NFET and PFET leakage monitors.

The body bias *offset* has exponential impact on performance in the sub- $V_{th}$  regime. However, Fig. 6 shows that energy consumption is nearly independent of  $V_{th}$  as long as the system remains in the sub- $V_{th}$  regime, supporting the derivation in [1]. Hence, the offset can be used to tune performance with minimal impact on energy.

With proper selection of differential and offset, we can address energy and performance variability due to systematic process variations. Fig. 7 shows that the mean  $V_{dd,limit}$  for 20 dies reduces from 221mV to 168mV (a 24% improvement) when a unique energy optimal differential is applied to each die as in Fig. 5, suggesting a dramatic improvement in noise margins. Fig. 8 shows energy and frequency measurements at  $V_{dd}$ =300 mV over the same 20 dies for 4 different cases. In the first case, body biases are tied to the appropriate  $V_{dd}$  and  $V_{ss}$  rails (zero body bias). In the remaining 3 cases, the energy optimal body bias differential is applied, and body bias offset is chosen with 5mV resolution to meet frequency constraints of 66kHz (worst case frequency in Case 1), 100kHz, and 160kHz. The table in Fig. 8 summarizes the data from Cases 1 through 4 when all dies run exactly at the target frequency (66, 100 or 160kHz). Applying a body bias at 66kHz virtually eliminates delay variability and reduces the standard deviation of energy from 22fJ to 14fJ. Furthermore, a wide range of performance targets can be met with only minimal energy implications by tuning the body bias offset, as demonstrated by Cases 3 and 4. With a target frequency of 160kHz (Case 4), a 2.4X worst-case performance improvement and a 5% average energy improvement are achieved as compared to Case 1.

Similarly, proper selection of differential and offset can be used to compensate for variations in temperature. Fig. 9 shows that performance varies by 9.4X and energy increases by 74% between T=0 and 80°C. By setting a constant differential as in Fig. 5 and tuning the offset at each temperature, frequency can be held nearly constant from T=0 to 80°C and the energy increase can be reduced from 74% to 50%, as shown in Fig. 9.

## Performance Control

We focus on four primary performance enhancement techniques:  $V_{dd}$  scaling, body biasing, gate length ( $L$ ) sizing, and gate width ( $W$ ) sizing. Fig. 10 compares  $V_{dd}$  scaling and body biasing as chip-level performance control techniques. Body biasing is clearly an energy-efficient alternative to  $V_{dd}$  tuning over the performance range shown since it allows PFET/NFET matching (Fig. 5) and leverages the insensitivity of energy to  $V_{th}$  (Fig. 6). However, since neither of these techniques can be easily applied at a block level, we also explore two gate sizing techniques. Improved drive strength is usually achieved by increasing  $W$ , but it can also be gained by increasing  $L$  in the sub- $V_{th}$  regime. Due to halo implants, reverse short channel effects lead to  $V_{th}$  reductions at increased  $L$ . In the technology stud-

ied, on-current is increased by 2.4X when  $L$  increases from 120 to 200nm at  $V_{dd}=300\text{mV}$ . This high sensitivity suggests that  $L$  increases may be used to gain drive strength more efficiently than  $W$  increases alone. We measure energy and frequency for 3 processor variants: 1) minimum gate sizes (Proc A), 2) gate sizes increased using a typical standard cell library (Proc B) and 3) gate sizes increased using a standard cell library incorporating increased  $L$  and  $W$  (Proc C). The cores in Procs B and C were sized with energy as the objective as in [7]. Selected gate sizes from a subsection of the ALU are noted in

### References

- [1] B. Zhai, et al., *DAC*, 2004.
- [2] B. Calhoun, et al., *ISLPED*, 2004.
- [3] L. Nazhandali, et al., *CASES*, 2005.
- [4] A. Wang, A. Chandrakasan, *ISSCC*, 2004.
- [5] M. Miyazaki, et al., *ISSCC*, 2002.
- [6] G. Ono, et al., *J. Solid-State Circuits*, 2003.
- [7] S. Hanson, et al., *ISLPED*, 2006.

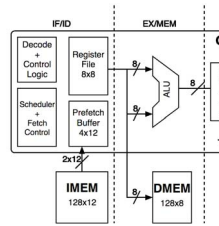


Figure 1: An 8-bit processor was implemented [3].

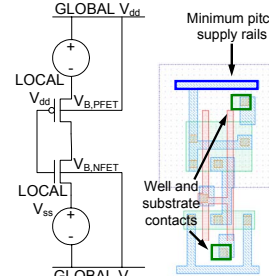


Figure 2: Body bias and power distribution schemes shown schematically

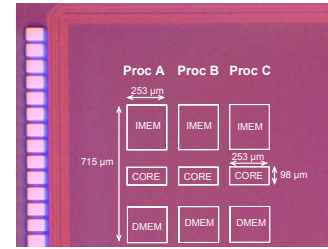


Figure 3: Die photograph high-lighting core and memory for 3 processor variants

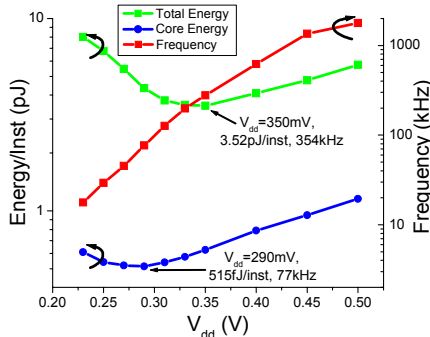


Figure 4: Energy and frequency measurements for an application with CPI~1.4

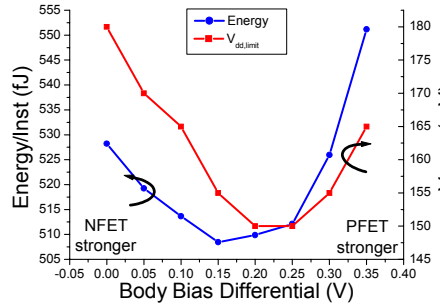


Figure 5: Energy and  $V_{dd,limit}$  as functions of body bias differential for a single die

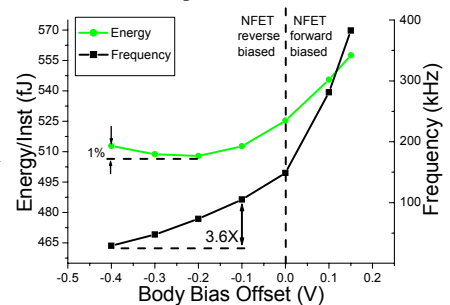


Figure 6: Energy and frequency as functions of body bias offset for a single die

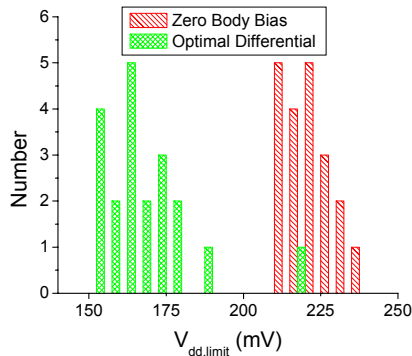


Figure 7:  $V_{dd,limit}$  distribution over 20 dies with and without body biasing

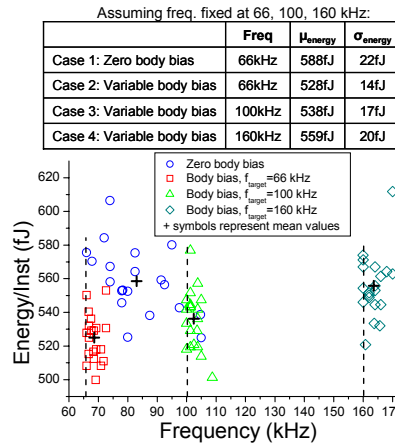


Figure 8: Energy and frequency distributions over 20 dies under various body bias schemes

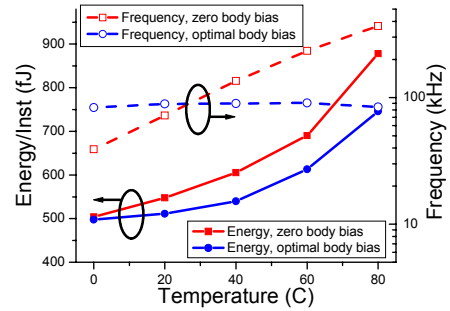


Figure 9: Energy and frequency temperature sensitivity for a single die with and without body biasing

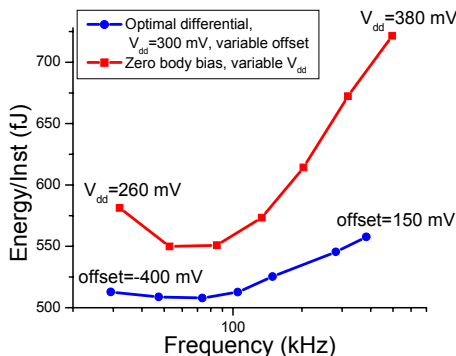


Figure 10: Energy-performance trade-off for variable body bias and variable  $V_{dd}$  systems

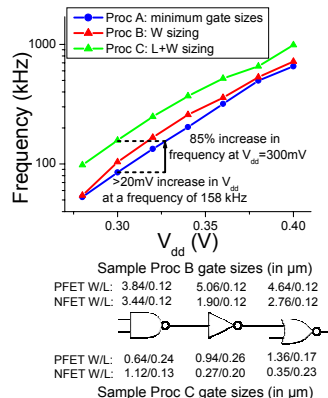


Figure 11: Frequency measurements for 3 core variants. Gate sizes along an ALU path shown.

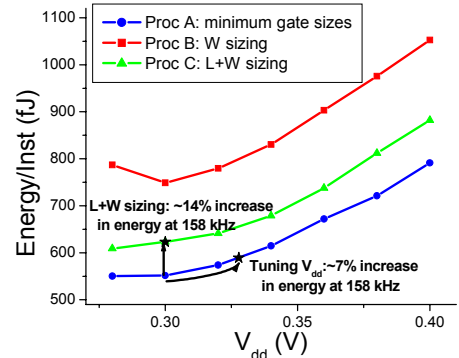


Figure 12: Energy measurements for 3 cores with different sizing schemes

Fig. 11 as an example. Proc C is both faster and more energy efficient than Proc B over the  $V_{dd}$  range shown, suggesting that  $L$  sizing is superior to  $W$  sizing. The use of increased  $L$  improves performance by 85% at  $V_{dd}=300\text{mV}$  for a 14% energy penalty compared to the case with minimum gate sizes, as shown in Figures 11-12. However, the frequency of Proc A can alternatively be increased by 85% for a ~7% energy penalty by increasing  $V_{dd}$  by 20-30mV, suggesting that  $L$  sizing is desirable only for block-level performance tuning.